Canadian Mineralogist
Vol. 28, pp. 55-66 (1990)

SERPENTINIZATION IN THE ARCHEAN KOMATIITIC ROCKS OF THE KUHMO GREENSTONE BELT, EASTERN FINLAND

SYLVAIN BLAIS AND BERNARD AUVRAY

Centre Armoricain d'Étude Structurale des Socles, Institut de Géologie, Université de Rennes, 35042 - Rennes Cedex, France

ABSTRACT

Within the Suomussalmi-Kuhmo-Tipasjärvi greenstone belt of Archean age in eastern Finland, there are numerous outcrops of serpentine-bearing rocks. Petrographic and mineralogical observations have led to the recognition of three stages of mineral growth during metamorphism: I) low-grade serpentinization, with dominant lizardite I culminating in the complete transformation of magmatic olivine; II) prograde metamorphism, leading to the appearance of a new generation of olivine associated with acicular antigorite, which shows an interpenetrating texture, and III) a renewed episode of low-grade serpentinization, corresponding to a partial conversion of metamorphic olivine to lizardite II. Stages I and III correspond to the development of lizardite with a mesh texture. During each stage of mineral growth, each serpentine phase shows a specific composition. Lizardite I is characterized by the presence of Al, Mn, Ca, Na, K, Cr and Ni, whereas lizardite II appears to be highly depleted in these elements. The variability of Fe^{2+} contents in lizardite II is probably related to the compositional characteristic of the metamorphic olivine. Antigorite is characterized by an enrichment in Al, Cr and Mg linked to the breakdown of chromite during the main phase of prograde metamorphism.

Keywords: serpentinization, komatiite, greenstone belt, Kuhmo, Archean, eastern Finland.

SOMMAIRE

Au sein de la ceinture archéenne de roches vertes de Suomussalmi-Kuhmo-Tipasjärvi (Finlande orientale) affleurent de nombreuses roches dans lesquelles abondent les minéraux serpentineux. Les observations minéralogiques permettent de mettre en évidence trois stades métamorphiques: I) serpentinisation de bas degré où domine la lizardite I, aboutissant à une transformation totale de l'olivine magmatique; II) métamorphisme prograde, conduisant à l'apparition d'une nouvelle génération d'olivine et au développement d'aiguilles d'antigorite à texture interpénétrée; III) nouvelle serpentinisation de bas degré correspondant à une altération partielle de l'olivine métamorphique en lizardite II. Le premier et le troisième stade correspondent à un développement de lizardite à texture maillée. La lizardite I est caractérisée par la présence d'éléments comme Al, Cr, Ni, Mn, Ca, Na et K, alors que la lizardite II en est totalement dépourvue. Cette dernière présente des teneurs en Fe^{2+} variables, en relation avec la nature même de l'olivine métamorphique. L'antigorite est caractérisée par une grande richesse en Al, Cr et Mg; cet enrichissement est lié à la déstabilisation de la chromite au cours de l'épisode métamorphique prograde principal (stade II).

Mots-clés: serpentinization, komatiite, ceinture de roches vertes, Kuhmo, Archéen, Finlande orientale.

INTRODUCTION

Serpentinization processes have long attracted the attention of numerous investigators, and the associated literature is abundant (*Canadian Mineralogist* 17, part 4, 1979). Studies have concentrated mainly on the mineralogy and crystallography of serpentine minerals, as well as on the mode of serpentine formation in various geological settings (Wicks & Whittaker 1977). Recently, the success of chemical analyses by microprobe methods has augmented the available data-base and led to a better understanding of the geochemistry of serpentinization processes.

The Archean greenstone belt of Suomussalmi-Kuhmo-Tipasjärvi (Blais *et al.* 1977, Taipale *et al.* 1980, Piirainen 1988, Blais 1989) is particularly well suited for the study of serpentine minerals, as the ultramafic rock-types have undergone a multistage history and are composed predominantly of serpentine. The different phases of serpentinization have been related to various stages of metamorphism (Piquet 1982, Blais 1989); this insight has led to the recognition of successive textural relationships and the interpretation of geochemical mobility. The present study of serpentine minerals is based on petrographic observations as well as detailed chemical analyses of the minerals concerned. It demonstrates the participation of spinel in the development of antigorite during one stage of metamorphism.

GEOLOGICAL SETTING

The three types of lithologic units classically described in Archean "granite-greenstone" belts (Windley & Bridgwater 1971) also are recognized in the Archean terranes of eastern Finland, where outcrops can be assigned as follows: a gneissic basement containing rocks of tonalitic, trondhjemitic and granodioritic composition ranging in age from 2.86

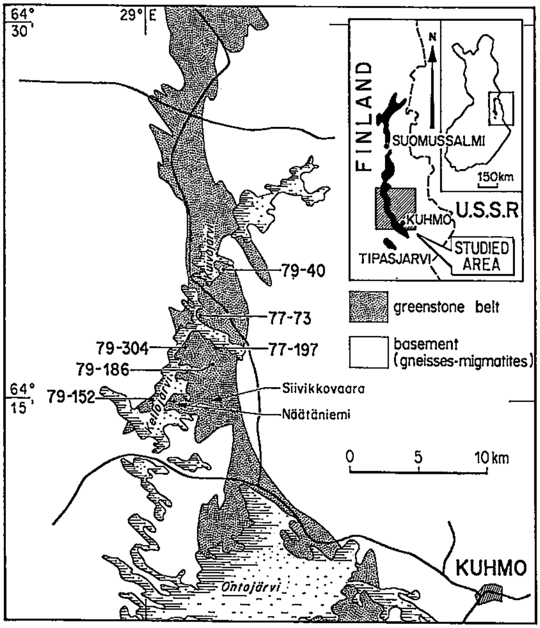

FIG. 1. Geological sketch map of the Kuhmo area (eastern Finland).

to 2.65 Ga (Martin *et al.* 1983, 1984), a greenstone belt dated at 2.65 Ga (Vidal *et al.* 1980) and extending over more than 200 km long from north to south but less than 20 km wide (see Fig. 1), calc-alkaline plutonic rocks younger than the greenstone belt and showing two episodes of intrusion, leading to porphyritic granodiorites emplaced at about 2.50 Ga, and pink granites dated at 2.41 Ga (Martin & Querré 1984).

The greenstone belt is composed mainly of basic and ultrabasic volcanic rocks that have been deformed (Bertrand *et al.* 1978) and metamorphosed under conditions of the greenschist or upper amphibolite facies (Piquet 1982, Taipale 1983, Blais & Auvray 1987). The various stages of growth of metamorphic minerals have been established from petrographic observations, particularly from the komatiites and associated rock-types. These different episodes are as follows: Stage I is characterized by low-grade serpentinization and complete transformation of the original magmatic olivine. Even without conclusive evidence, this episode can probably be related to hydrothermal alteration during emplacement of the lavas. During Stage II, prograde metamorphism led to the crystallization of olivine with interpenetrating needles of serpentine. This episode corresponds to the regional metamorphism affecting the belt. Physical conditions can be estimated at 2 kbars total pressure, 440–485°C (according to thermodynamic data in Trommsdorff & Evans 1977) for serpentine–olivine assemblages, which corresponds to the greenschist facies; olivine-bearing amphibolites yield significantly higher temperatures, in the range 490–535°C (Blais & Auvray 1987), which is near the lower limit of the amphibolite facies. In Stage III, an episode of renewed low-grade serpentinization corresponds to the partial transformation of metamorphic olivine. This stage can be interpreted as either the climax of retrograde regional metamorphism or, alternatively, the influence of the Karelian orogeny (*cf.* biotite Rb–Sr dates around 1.76 Ma: Vidal *et al.* 1980, Martin 1985). These three stages of growth of the serpentine mineral are investigated in the present study using textural and mineralogical data, in order to interpret the mechanisms of chemical exchange among the different phases.

Ultramafic rocks show an irregular distribution across the belt, but are particularly abundant in the central region (Kuhmo), where most of the samples for the present study were collected, mainly near lakes Kellojärvi and Kuivajärvi, which are situated north of Siivikkovaara area (Fig. 1). This area is characterized by the presence of abundant spinifex-textured komatiite flows, pillow lavas and volcanic breccias (Hanski 1980).

Serpentine minerals were studied in samples of metacumulate rocks that show replacement of the original igneous textures with metamorphic assemblages; in certain cases, a magmatic cumulate texture is preserved. The mineralogy of these rocks (serpentinites) is presented in Table 1, and whole-rock chemical compositions are presented in Table 2.

TEXTURES OF SERPENTINE MINERALS IN METACUMULATE ULTRABASIC ROCKS OF THE KUHMO REGION

The present description of serpentine textures is based on the classification of Wicks & Whittaker (1977), who proposed three types: (1) pseudomorphic textures, in which serpentine minerals follow the habit and boundaries of primary minerals (mainly olivine), (2) nonpseudomorphic textures, in which original textures are not preserved, and serpentine minerals are formed at the expense of pre-existing assemblages of pseudomorph material, and (3) serpentine veins. The first two types are common within the Kuhmo belt, whereas veins are rare and will not be mentioned further.

Pseudomorphic textures

The serpentine minerals are formed exclusively at the expense of olivine in this suite. The Kuhmo metacumulates show two types of pseudomorph after olivine: mesh texture and hourglass texture.

TABLE 1. MINERAL ASSOCIATIONS IN KUHMO GREENSTONE BELT

Rock type	Sample number	Mineralogy
Serpentinite with magmatic olivine relics	79-152	Chlorite, (± pyroxene), serpentine, ± brucite, opaque minerals.
Amphibolite serpentinite with hourglass texture	79-186	Serpentine, chlorite, tremolite, dolomite, opaque, ± pyroxene.
Olivine serpentinite	77-73, 79-304, 77-197	Olivine, serpentine, magnetite.
Olivine amphibolite	79-40	Tremolite, chlorite, opaque minerals, olivine, serpentine.

For location of samples, see Fig. 1.

The pseudomorphic mesh texture is developed during hydration of olivine, where the olivine can be either magmatic or metamorphic, and is widely described by many authors (*e.g.*, Moeskops 1977, Wicks *et al.* 1977, Wicks & Whittaker 1977, Maltman 1978). The mesh texture is classically described as being composed of two parts; the core and the rim make up the mesh itself. In the Kuhmo region, the core can be made up of olivine, brucite or a mixture of serpentine and brucite that shows a rusty yellow color in transmitted light. Various examples of mesh core are shown in Figures 2A, B and C. Serpentine rims are spectacularly well developed in mesh textures with an olivine core. The most commonly observed fiber structure (so-called bipartite fibers) consists of two main parts separated by a thin band of very fine-grained fibrous material (see Fig. 2C). Wicks & Zussman (1975) have shown that this type of structure is generally made up of lizardite. The chemical data in Table 3 are consistent with the presence of lizardite in the mesh-textured serpentine.

The mesh textures are developed at the expense of both magmatic and metamorphic olivine (Blais & Auvray 1987). Magmatic olivine is entirely transformed to a mixture of serpentine and brucite. In contrast, metamorphic olivine is only partly serpentinized. These two generations of serpentine (Lizardite I and II) are formed from two successive generations of olivine that grew during different phases of mineral growth; the two types of serpentine are discussed separately in the section on chemical composition of serpentine-group minerals.

The pseudomorphic hourglass texture is described by Wicks *et al.* (1977) and Laurent & Hébert (1979) and has been found in several Archean serpentinites of the present study (see Fig. 2D). It is developed from magmatic olivine and, in contrast to the serpentines of the mesh-textured metacumulates, is composed of fibrous antigorite. This may be interpreted as resulting from recrystallization of lizardite I.

TABLE 2. WHOLE-ROCK COMPOSITION OF SERPENTINITES

	79-152	79-186	79-304	77-197	79-40
SiO_2 wt.%	38.00	40.70	35.63	37.98	40.65
Al_2O_3	2.48	4.16	1.15	1.59	4.78
Fe_2O_3	6.17	9.26	9.56	6.40	5.35
FeO	n.d.	n.d.	3.34	2.66	4.86
MnO	0.12	0.16	0.25	0.22	0.17
MgO	38.52	31.58	38.22	39.70	29.43
CaO	0.03	3.75	tr	tr	4.77
Na_2O	tr	tr	tr	tr	0.23
K_2O	tr	tr	tr	tr	tr
TiO_2	0.12	0.21	0.07	0.10	0.31
P_2O_5	0.05	0.04	tr	tr	0.05
L.O.I.	13.84	10.28	11.18	11.72	9.12
	99.33	100.14	99.40	100.37	99.72
Ni ppm	2452	1805	1687	2327	1601
Cr	1525	3348	3791	3404	2859
Co	108	107	119	125	103
V	49	75	36	33	124

The major elements, except for Na, Mg and Fe^{2+}, were determined by the XRF method. Na and Mg were determined by the atomic absorption method, and Fe^{2+} by colorimetry.

Nonpseudomorphic textures

The serpentine minerals do not follow the form or habit of pre-existing phases. However, it should be pointed out that nonpseudomorphic serpentines do not entirely obliterate the magmatic textures of the metacumulates; in fact, olivine "ghosts" can be

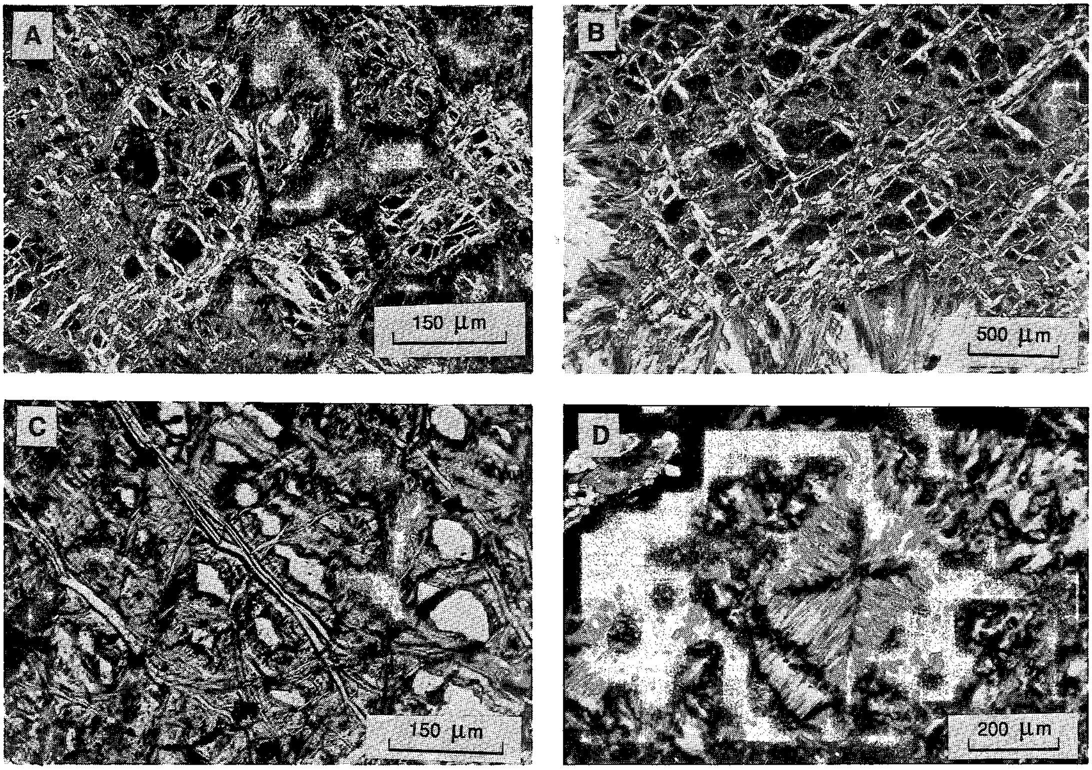

FIG. 2. Pseudomorphic serpentine textures. (A) Mesh texture after magmatic olivine: core is lizardite + brucite, rims are lizardite I. Sample 79–152. (B) Mesh texture: core is metamorphic olivine, rims are lizardite II. Antigorite at left and bottom. Sample 77–73. (C) Crystal of metamorphic olivine cut by lizardite II (bi-partite fiber). Sample 77–194. (D) Hourglass texture: lizardite I replaced by antigorite. Sample 79-186.

picked out by the arrangement of opaque minerals (Blais & Auvray 1987). Following Wicks & Whittaker (1977), two types of nonpseudomorphic texture can be recognized in the present material. In the interlocking type, the serpentine grains show irregular to equant outlines. In the interpenetrating type, elongate laths exhibit a habit that ressembles a nematoblastic texture. The interpenetrating texture is the more common one. Serpentine laths commonly show no preferred orientation (Fig. 3A) and may display large rosette-shaped bundles (Fig. 3B).

X-ray diffraction and differential thermal analyses clearly show that all the serpentine making up these nonpseudomorphic textures is composed of antigorite (*cf.* Whittaker & Zussman 1956, Boudier 1971).

Interpretation of the textures

The investigation of serpentine mineral textures in the Kuhmo region has led to the recognition of a sequence of episodes of mineral growth, as summarized in Figure 4. At first, crystals of magmatic olivine were partly or completely serpentinized, giving rise to classic mesh textures made up of lizardite I, and probably certain hourglass textures, which were initially composed of this type of serpentine. Stage-I serpentinization took place during retrograde metamorphism. Later, the low-grade serpentine minerals were recrystallized as antigorite. The pseudomorphic textures of stage I are mostly replaced by nonpseudomorphic textures. Hourglass textures of antigorite may represent an intermediate stage in which original shapes of primitive olivine were preserved despite recrystallization (Fig. 2D). With continuing recrystallization, the hourglass-textured serpentine was converted to nonpseudomorphic antigorite. This stage of antigorite growth (stage II) can be assigned to prograde metamorphism, and led to the development of metamorphic olivine and pyroxene. Finally, the metamorphic olivine is itself serpentinized (stage III), giving rise to new mesh textures of lizardite II surrounding an olivine core.

CHEMICAL COMPOSITION OF THE SERPENTINE MINERALS

Results of microprobe analyses (Table 3) are quoted as average compositions based on *n* analyses in each case. Compositions of metamorphic olivine also are included in this table. The compositions presented in Table 3 correspond to the different tex-

TABLE 3. CHEMICAL COMPOSITION* OF SERPENTINE AND OLIVINE

Sample N°	79-152						79-186				77-73			
	Lizardite I		Antigorite		Antigorite of the Hourglass texture		Antigorite		Antigorite		Metamorphic Olivine		Lizardite II	
n		25		16		16		10		24		24		21
SiO_2	38.21	(2.26)	41.04	(0.73)	39.61	(1.22)	40.29	(0.50)	42.08	(1.40)	42.04	(0.33)	36.95	(2.82)
Al_2O_3	0.21	(0.14)	3.22	(0.76)	4.68	(1.59)	4.17	(0.36)	1.35	(0.47)	0.01	(0.01)	0.01	(0.02)
FeO	5.54	(3.34)	2.93	(0.29)	7.01	(0.31)	7.29	(0.19)	1.86	(0.41)	4.30	(0.28)	3.25	(1.53)
MnO	0.25	(0.40)	0.08	(0.07)	0.11	(0.08)	0.14	(0.04)	0.12	(0.22)	0.41	(0.10)	0.17	(0.11)
MgO	39.17	(1.86)	39.46	(0.50)	35.04	(0.36)	35.64	(0.22)	41.33	(0.89)	54.29	(0.68)	42.93	(1.58)
CaO	0.06	(0.04)	0.01	(0.02)	0.01	(0.01)	-	-	-	-	0.01	(0.01)	-	-
Na_2O	0.03	(0.03)	0.02	(0.03)	-	-	0.02	(0.02)	-	-	-	-	0.01	(0.01)
K_2O	0.12	(0.06)	0.04	(0.03)	0.02	(0.02)	0.03	(0.02)	-	-	0.01	(0.02)	0.01	(0.01)
Cr_2O_3	0.12	(0.17)	0.21	(0.21)	0.32	(0.17)	0.16	(0.10)	0.30	(0.28)	0.02	(0.04)	0.02	(0.05)
TiO_2	0.09	(0.32)	0.02	(0.02)	0.02	(0.02)	0.02	(0.02)	0.02	(0.03)	0.01	(0.02)	0.01	(0.02)
NiO	0.32	(0.14)	0.21	(0.08)	0.15	(0.08)	0.20	(0.10)	0.07	(0.06)	0.29	(0.10)	0.18	(0.08)
	84.12		87.24		86.97		87.96		87.13		101 39	Fo_{95}	83.54	

Sample N°	79-304						77-197				79-40			
	Antigorite		Metamorphic Olivine		Lizardite II		Antigorite		Metamorphic Olivine		Metamorphic Olivine		Lizardite II	
n		14		18		5		14		12		14		12
SiO_2	42.41	(1.01)	42.75	(0.60)	37.22	(2.45)	41.39	(0.72)	41.41	(0.30)	38.96	(0.14)	38.83	(1.28)
Al_2O_3	1.39	(0.40)	0.01	(0.01)	-	-	2.09	(0.56)	0.01	(0.02)	0.02	(0.02)	0.14	(0.36)
FeO	1.54	(0.20)	3.72	(0.28)	2.65	(0.86)	2.32	(0.36)	5.43	(0.27)	21.29	(0.28)	8.24	(2.69)
MnO	0.06	(0.04)	0.52	(0.18)	0.24	(0.07)	0.09	(0.11)	0 53	(0.09)	0.38	(0.05)	0.22	(0.15)
MgO	39.98	(0.60)	52.97	(0.44)	41.22	(1.05)	39.89	(0.36)	52.51	(0.45)	40.06	(0.34)	37.56	(1.80)
CaO	0.01	(0.01)	0.01	(0.02)	0.03	(0.04)	0.02	(0.02)	0.01	(0.01)	0.01	(0.01)	0.06	(0.02)
Na_2O	-	-	-	-	0.01	(0.01)	-	-	-	-	0.01	(0.02)	0.01	(0.02)
K_2O	0.02	(0.02)	0.01	(0.01)	-	-	0.02	(0.02)	0.01	(0.01)	0.01	(0.01)	0.04	(0.03)
Cr_2O_3	0.25	(0.18)	0.02	(0.02)	-	-	0.29	(0.24)	0.01	(0.02)	0.04	(0.03)	-	-
TiO	0.02	(0.02)	0.01	(0.02)	-	-	0.01	(0.02)	0.01	(0.01)	-	-	-	-
NiO	0.06	(0.07)	0.24	(0.10)	0.26	(0.10)	0.11	(0.06)	0.37	(0.01)	0.23	(0.09)	0.21	(0.12)
	85.14		100.26	Fo_{96}	81.64		86.23		100.32	Fo_{94}	101,01	Fo_{77}	85.31	

* Obtained by Automatic microprobe (Microsonde Camebax, "Ouest" Brest) operating conditions 15 KV, 10 nA, counting time 6s., n corresponds to the number of point analyses included in the average ; ( ) = standard deviation; Fo = molecular proportion of forsterite. Standard are Wollastonite (Si-Ca), Al_2O_3 (Al), Fe_2O_3 (Fe), Rhodonite (Mn), Forsterite (Mg), Albite (Na), Orthoclase (K), Cr_2O_3 (Cr), TiO_2 (Ti) and NiO (Ni).

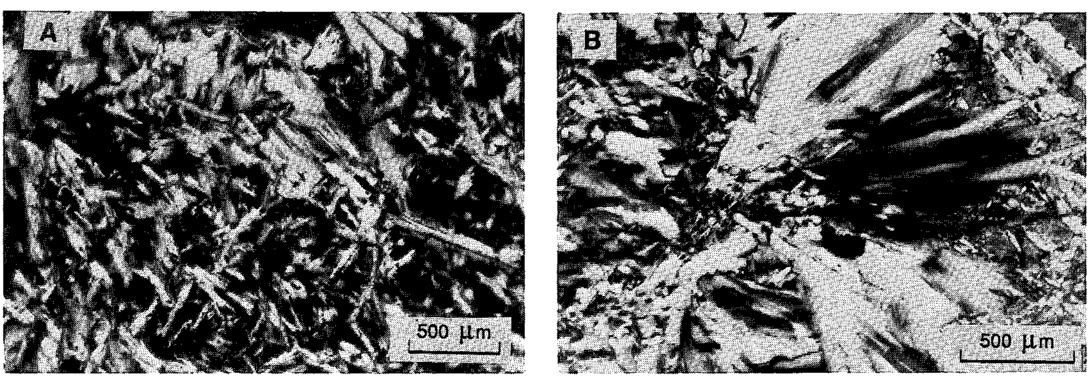

FIG. 3. Nonpseudomorphic textures. (A) Interpenetrating texture made up of antigorite laths. Sample 77-73. (B) Interpenetrating texture composed of rosette-shaped bundle of antigorite. Sample 77-73.

Stage I	Stage II	Stage III
Serpentinization I (retromorphic)	Serpentinization II (prograde metamorphism)	Serpentinization III (retromorphic)
Magmatic olivine		Metamorphic olivine
Lizardite I + Brucite	Antigorite	Lizardite II
Pseudomorphic texture	non-pseudomorphic texture	pseudomorphic texture
low values : Al, Cr, Ni, Mn, Ca, Na, K.	enriched in Al, Cr.	variable amount of Fe no Al, Cr, K.

FIG. 4. Different stages of successive serpentinization and chemical characteristics of serpentinite minerals.

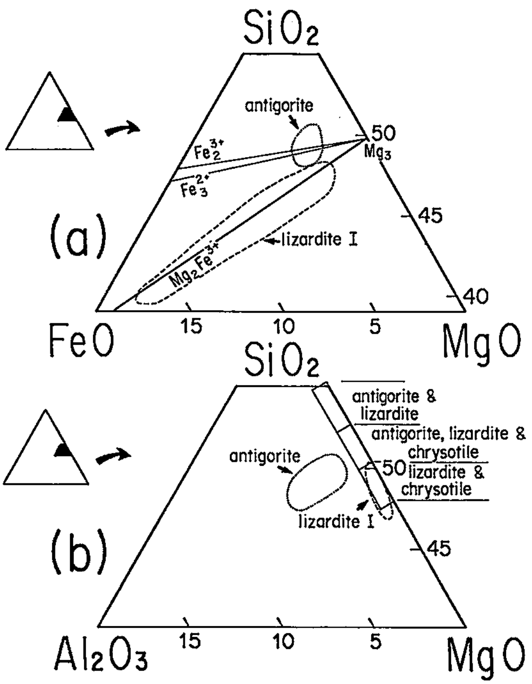

FIG. 5. MgO – FeO – SiO_2 (a) and MgO – Al_2O_3 – SiO_2 (b) diagrams: microprobe data for antigorite and lizardite I (serpentinite 79–152) are shown as dotted and dashed envelopes, respectively. See text for explanation.

tural types previously described: mesh-textured serpentines from stage I and III, hourglass serpentine and nonpseudomorphic serpentine with an interpenetrating texture (stage II). These chemical compositions lead to an interpretation of compositional variation in terms of redistribution of elements during the successive phases of serpentinization and metamorphism. All these compositions are plotted on the triangular diagrams MgO-SiO_2-FeO and MgO-SiO_2-Al_2O_3 (Figs. 5, 6, 7), used by Wicks & Plant (1979).

The association of mesh-textured lizardite I, belonging to stage I, and antigorite from stage II displaying interpenetrating texture is present in a clinopyroxene-bearing serpentinite (Sample 79–152). Chemical data relating to this sample are given in Table 3, and the compositional fields are indicated on Figures 5a and 5b. It is immediately apparent that the lizardite I phase is heterogeneous; Fe^{2+} is highly variable and shows a linear trend from 3 to 15% FeO (Fig. 5a). Al_2O_3 contents are much lower than 1%, although significantly greater than the detection limit. Furthermore, the results show low but significant concentrations of Mn, Ca, Na, K, Cr, Ti and Ni. In the same sample, the antigorite laths that show an interpenetrating texture have FeO contents that are more tightly grouped (*ca.* 3–4%) than those of lizardite I, and SiO_2 contents are higher. However, the main distinguishing feature between lizardite I and antigorite is the Al_2O_3 content (see Fig. 5b), which ranges from 2 to 5% in the antigorite. Compositions of lizardite I and antigorite, corresponding to two different textural sites in the same sample of serpentinite, can be clearly distinguished by use of the MgO-SiO_2-Al_2O_3 diagram (Fig. 5b).

Another association groups together hourglass-textured (antigorite) serpentine of stage II with antigorite laths of the same generation. Such an association is observed in a sample of amphibole-bearing serpentine (sample 79-186, Figs. 6a, b).

Chemical data corresponding to this sample are given in Table 3; the two serpentine species show closely similar compositions, and the representative points are grouped (see Fig. 6a in particular). The hourglass-textured pseudomorphs show much more variable Al_2O_3 contents than the antigorite laths (see Fig. 6b) and follow a linear trend from 4 to 9% Al_2O_3. The associated antigorite is much more homogeneous, showing Al_2O_3 contents arounds 4.17%.

A third type of association groups together non-pseudomorphic antigorite (stage II) associated with lizardite II that is derived from the retrograde serpentinization of metamorphic olivine (stage III). As summarized in Figure 4, metamorphic olivine was developed within a matrix of antigorite needles during the main phase of regional metamorphism. Such olivine can be characterized by textural and chemical criteria that indicate a metamorphic origin (Blais & Auvray 1987). During a phase of retrograde metamorphism (stage III), the olivine was partly transformed to lizardite II. Of the four samples studied showing metamorphic olivine (Table 3), three contain olivine with a very high Mg content and one sample contains olivine with lower Mg.

In two samples of serpentinite with a highly magnesian olivine (77–73 and 79–304; Fo_{95-96}), antigorite and lizardite II have been analyzed. In one sample (77–197, Fo_{94}) that contains olivine similar to the two other samples, only the antigorite has been analyzed. All the results are reported in Table 3. In all three samples, the antigorite has a near-constant composition characterized by high SiO_2 contents (*ca.* 42%), Al_2O_3 in the range 1.40–2%, Cr_2O_3 contents near 0.3%, and low concentrations of NiO (< 0.11%). The lizardite II phase is relatively depleted in SiO_2 with respect to antigorite but is enriched in Mg, Mn, Fe and Ni; however, the main chemical characteristic of lizardite II is the total lack of Al (Fig. 7b), Cr, Ti and K.

One serpentine sample (79–40) contains less magnesian metamorphic olivine (Fo_{77}), associated with lizardite II having the highest measured Fe^{2+} contents (3.30%–14.50% FeO; Fig. 6a). This occurrence illustrates clearly the compositional relationship between Fe^{2+} content in metamorphic olivine and in the products of its replacement.

Compositions of serpentine minerals in different textural associations (Fig. 4) can be summarized as follows: (1) mesh-textured lizardite I is derived from the serpentinization of magmatic olivine and is characterized by low contents of Al, Cr, Ni, Mn, Ca, Na and K. Blais & Auvray (1987) showed that the Fe contained in the magmatic olivine is distributed among the serpentine minerals, brucite and the separate opaque phase found at the boundaries of the original olivine; (2) the hourglass-textured pseudomorph material and the matrix serpentine showing interpenetrating texture have antigorite compositions

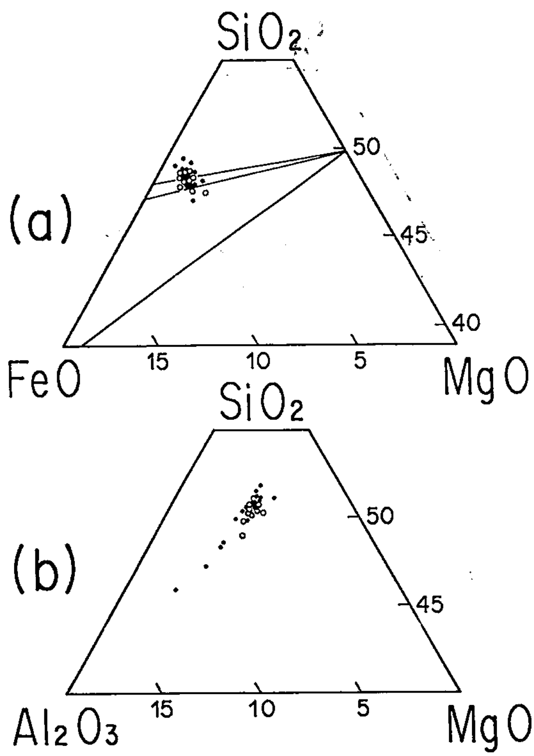

FIG. 6. MgO – FeO – SiO_2 (a) and MgO – Al_2O_3 – SiO_2 (b) diagrams: microprobe data for antigorite in sample 79–186. (• Hourglass texture; o interpenetrating texture).

and are formed during prograde metamorphism (stage II). They are clearly enriched in Al and show significant traces of Cr; (3) mesh-textured lizardite II is formed from the breakdown of metamorphic olivine during stage III. This lizardite II is characterized by variable Fe^{2+} contents, reflecting the composition of the metamorphic olivine, and a total lack of elements such as Al, Cr and K.

Figure 8 illustrates the MgO and SiO_2 contents of the four textural types of serpentine minerals. Interpenetrating antigorite is richer in SiO_2 than the lizardite I developed after magmatic olivine, whereas their MgO contents overlap. The variation in MgO for these two types of serpentine is inversely correlated with FeO content. The hourglass antigorite from sample 79–186 has a SiO_2 content that overlaps broadly with stage-I and stage-II serpentines, and shows an inverse correlation in Al content. The high concentrations of Fe^{2+} (7% FeO) observed in the hourglass antigorite are probably related to the low MgO contents (35%) compared with other examples of antigorite and lizardite

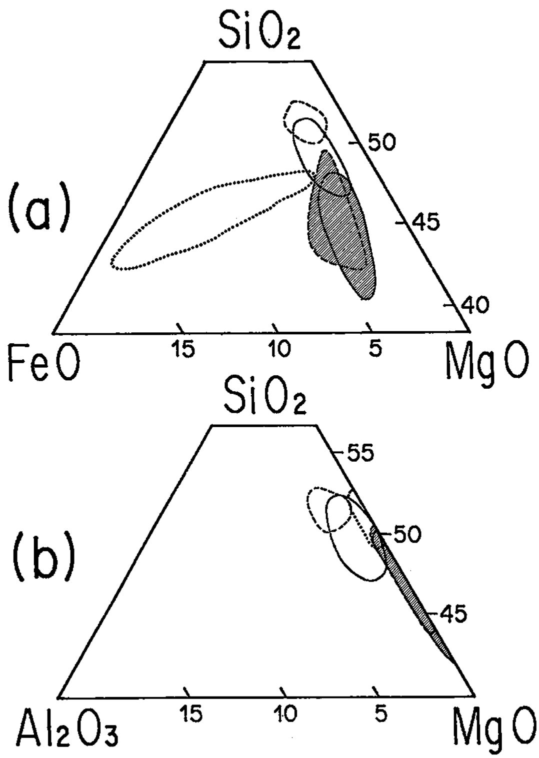

FIG. 7. MgO - FeO - SiO_2 (a) and MgO - Al_2O_3 - SiO_2 (b) diagrams: microprobe data for serpentine minerals (1) from highly magnesian olivine serpentinite (——— 77–73 and ---- 79–304) in which the antigorite corresponds to the fields outlined, and lizardite II corresponds to hachured envelopes, and (2) from less magnesian olivine amphibolite (...... 79–40) in which lizardite II alone has been analyzed.

studied here. This difference may be due to the alteration of a pre-existing magmatic olivine that was poor in the forsterite component (see low MgO content of sample 79–186 in Table 2).

The lizardite II derived from the breakdown of highly magnesian olivine (samples 77–73 and 79–304) has a significantly higher MgO content than any of the previously described serpentine minerals. In order to compare metamorphic olivine compositions among rocks of similar bulk-composition, sample 79–40 is excluded from the present discussion owing to its unusually low MgO content (see Table 2). These lizardite II data can be explained by the fact that metamorphic olivine, which itself is altered to lizardite II, is more magnesian than the initial magmatic olivine. During stage-I serpentinization of the initial olivine, Fe is tied up in the form of magnetite; this leads to less Fe available during stage-II prograde growth of olivine from antigorite. In this way, metamorphic olivine has a low content of Fe because of recrystallization in an environment in which the Fe is not free to move (Hietanen 1977, Zhang 1981, Blais & Auvray 1987).

Chemical Behavior During the Three Stages of Serpentinization

Having established the particular characteristics of each stage of serpentinization, it is possible to link the observed chemical variations with geochemical processes that may have operated during each stage.

Serpentinization I

During the serpentinization of magmatic olivine, elements are redistributed among the different new minerals. Fe derived from the olivine enters the serpentine structure as well as the associated brucite and magnetite. Analyses of lizardite I show high FeO contents, varying between 3 and 15%; these compositions are comparable to the data of Wicks & Plant (1979). These authors have shown that lizardite compositions vary as a function of the degree of serpentinization. The compositions are rich in Fe^{2+} and highly heterogeneous at low grade; at a higher grade, FeO values are low and homogeneous. Lizardite I contains significant traces of Mn, Ni, Ca, K, Na, Al and Cr. These components are inherited from magmatic olivine which, however, do not occur as fresh relics in the samples studied. In particular, Ni, Cr and Al are present in olivine from Archean komatiites (Arndt *et al.* 1977, Nesbitt 1971) as well as more recent ones (Echeverria 1980). Golightly & Arancibia (1979) have shown that the concentrations of these elements in lizardite derived from the alteration of olivine can be identical to those observed in the original minerals.

Serpentinization II

The second generation of serpentine minerals is composed of antigorite, which has formed at the expense of low-temperature serpentine phases (lizardite I). The coexistence of antigorite and lizardite I is only observed in one sample (79–152, see Fig. 5). Recrystallized antigorite has a Fe^{2+} content close to that measured in the more magnesian lizardite I (*i.e., ca.* 3% FeO). In contrast, Al is clearly enriched in antigorite, including the hourglass-textured serpentine (sample 79–186). We propose that this Al enrichment is linked to the breakdown of spinel in the metacumulates.

In the present study, spinel grains were analyzed (Table 4) using an electron microprobe in three samples: 79–152, serpentine with "ghosts" of totally altered magmatic olivine, 79–186, serpentinite with an hourglass texture, and 77–73, serpentinite with metamorphic olivine. Included in this discussion is sample S-3, corresponding to a metamorphic-olivine-bearing amphibolite from the Suomussalmi region (north of Kuhmo).

Representative compositions of spinel, reported in Table 4, are variable from one sample to another and even within individual grains (commonly zoned). The core is much richer in Cr than the rim, despite differences in absolute concentration from sample to sample. The Cr decrease from core to rim is correlated with a decrease in Mg, Mn, Ti and Al, and an increase in Fe. The compositions range from ferrichromite (core) to chromiferous magnetite (rim). The compositional field of the chromite from stratiform intrusive bodies and Alpine-type ophiolites has been defined in terms of Fe total *versus* Cr_2O_3 (Thayer 1970). All the present spinel compositions fall outside these discriminant fields (Piquet 1982). The chemical data indicate that the spinel in the rocks studied is distinct in its total lack of Al, even in the more Cr-rich grains. A single grain (sample S-3, Table 4) is much richer in Cr and Al (45.42% Cr_2O_3, 9.76% Al_2O_3) and corresponds to chromite typical of a stratiform complex, despite a rather low Al content.

In comparison with the magmatic spinel in komatiites from Ontario (Arndt *et al.* 1977) and Zimbabwe (Nisbet *et al.* 1977), the Kuhmo population is not compatible with a magmatic origin. In fact, the magmatic chromite compositions reported in Table 4 have higher Al (*ca.* 13% Al_2O_3), Mg (12% MgO) and Cr (52% Cr_2O_3) contents than even the Suomussalmi chromite (sample S-3), which is closest to a possible primary composition. Thus, the original igneous chromite of the Kuhmo belt, preserved as relics in only one sample, have been transformed into ferrichromite and chromiferous magnetite during the various stages of serpentinization and metamorphism. The transformation from chromite to ferrichromite is accompanied by complete elimination of Al from the spinel structure and slight loss of Cr and Mg. Further evolution toward chromiferous magnetite is accomplished by progressive substitution of Cr by Fe^{3+}. The Cr, Al and Mg diffuse toward the grain boundary, whereas Fe^{3+} migrates toward the core. The very low Mg contents and almost negligible Al observed in zoned grains of spinel having a marked variation in Cr suggest a greater mobility for Mg and Al with respect to Cr. This conclusion is in agreement with the findings of Springer (1974), Bliss & MacLean (1975), Frost (1975) and Pinsent & Hirst (1977), who have interpreted such a process in terms of oxidation of the original igneous spinel.

In this way, the Al enrichment observed in antigorite (including hourglass-textured pseudomorphs) can be explained by loss of Al from the chromite during alteration and its fixation in the serpentine structure. The relative mobility of Cr and

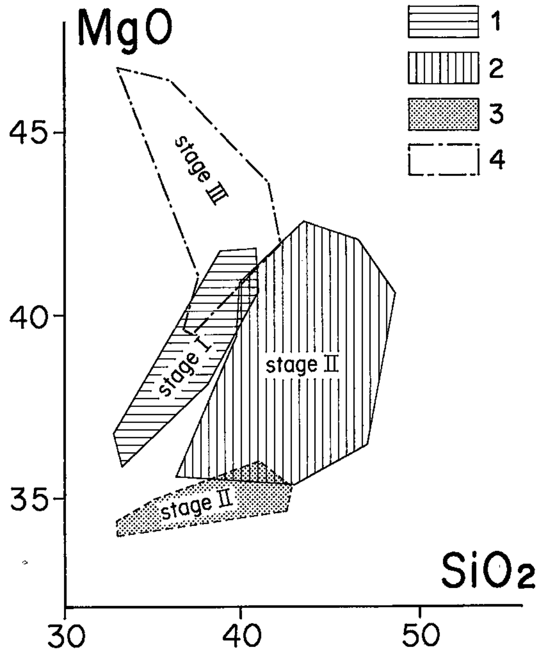

FIG. 8. MgO and SiO_2 compositional fields for the different types of serpentine minerals formed during stage I, II and III. Field 1: lizardite I after magmatic olivine; field 2: antigorite with interpenetrating texture; field 3: antigorite with hourglass texture; field 4: lizardite II after metamorphic olivine.

Mg is less important, but these elements are nevertheless concentrated into antigorite more than in magmatic olivine. However, it is difficult to interpret all the available data in terms of relative mobility during serpentinization, as whole-rock compositions cover a wide range. These igneous rocks, which formed by a process of fractional crystallization (Blais *et al.* 1978, Jahn *et al.* 1980), contain olivine that shows decreasing Mg contents as a function of increasing degree of fractional crystallization. The initial olivine compositions must influence the composition of serpentine minerals that are derived from the alteration of olivine-bearing igneous rocks.

Serpentinization III

The prograde metamorphism of ultrabasic cumulate rocks of the Kuhmo region has been shown to lead to the growth of metamorphic olivine in crystals up to several cm across. These grains have variable forsterite component (Fo_{96-77}), reflecting variations in whole-rock composition. During retrograde metamorphism, the more magnesian olivine (Fo_{94-96}) gives rise to highly magnesian serpentine minerals (*i.e.*, lizardite II, see Table 3), with

TABLE 4. CHEMICAL ANALYSES OF CHROMITE

Sample n°	79-152 Core					Rim	79-186 Core				Rim
SiO_2	0.03	0.11	0.01	0.01	-	-	-	0.17	-	-	0.02
Al_2O_3	0.26	0.27	0.23	0.20	-	0.02	0.17	0.22	0.15	-	-
Fe_2O_3	30.13	31.04	31.37	33.50	55.72	62.76	35.44	35.96	39.94	57.30	62.89
FeO	26.74	25.72	25.83	26.63	27.57	28.72	29.17	29.39	29.28	30.62	30.47
MnO	0.79	1.11	1.27	0.99	0.54	0.16	1.64	1.59	1.52	0.49	0.24
MgO	2.29	2.50	2.50	2.32	1.32	0.80	0.29	0.22	0.09	0.03	0.01
CaO	-	-	-	-	-	0.01	-	-	-	0.02	0.02
Na_2O	0.06	0.02	-	-	-	-	0.11	0.09	0.10	-	0.09
K_2O	-	0.01	-	0.01	-	0.04	0.06	0.01	0.01	-	-
TiO_2	1.87	1.75	1.49	1.81	1.41	0.66	0.84	0.48	0.24	0.14	0.01
Cr_2O_3	36.81	35.83	36.40	34.30	12.53	6.52	32.32	32.51	28.04	11.59	6.57
NiO	0.24	0.60	0.60	0.48	1.20	1.30	0.05	0.45	0.25	0.15	0.48
	99.22	98.96	99.70	100.25	100.29	100.99	100.09	101.09	99.62	100.34	100.80

Sample N°	77-73 Core			Rim	S-3 Core	Chromite from komatiites 1	2	3
SiO_2	-	-	-	0.03	-	-	0.71	0.55
Al_2O_3	0.05	0.08	0.12	-	9.76	13.9	13.5	11.69
Fe_2O_3	32.78	33.32	32.20	63.97	11.63	7.03	-	-
FeO	21.53	20.65	20.92	26.76	28.06	27.9	15.9	21.71
MnO	3.27	3.58	3.78	0.60	1.22	0.52	0.30	0.44
MgO	4.18	4.12	4.03	1.64	2.49	4.20	14.4	12.00
CaO	-	-	-	-	-	-	0.05	0.11
Na_2O	0.01	0.08	-	-	-	-	-	-
K_2O	0.01	-	0.02	-	-	-	-	-
TiO_2	0.99	1.13	1.06	0.26	0.31	0.45	0.31	0.32
Cr_2O_3	36.95	35.46	36.79	4.55	45.42	46.8	53.5	51.63
NiO	0.34	0.49	0.46	0.79	-	-	-	0.12
	100.11	98.91	99.38	98.60	98.89	100.80	98.70	98.57

1) Chromite from spinifex-textured komatiites, Fred's Flow, Arndt et al. (1977).

2) Chromite from flow-top breccia, Fred's Flow, Arndt (1977).

3) Chromite from spinifex rocks - SF 134 - Nisbet et al. (1977).

homogeneous Fe^{2+} contents. In contrast, the less magnesian olivine (Fo_{77}) is transformed into serpentine minerals with Fe-rich, heterogeneous compositions. In this case, the same explanation given for the composition of lizardite I can be invoked for lizardite II: with increasing degree of serpentinization, the serpentine minerals become more magnesian.

However, lizardite II can be distinguished from lizardite I in having almost no Al, Cr and K. Furthermore, these components also are absent in the metamorphic olivine. This could be taken as indirect evidence that lizardite I, containing significant traces of Al, Cr and K, is in fact derived from the alteration of magmatic olivine. Thus the chemical composition and textural relationships of lizardite can be used to determine whether this phase is derived from the alteration (retrograde or otherwise) of magmatic or metamorphic olivine.

Conclusion

From a combined study of textural relationships and chemical composition of rocks and minerals, it has been possible to recognize three successive generations of growth of serpentine minerals in komatiitic metacumulates of the Archean greenstone belt of Kuhmo. Stage-I and Stage-III serpentinizations (corresponding to the generation of lizardite I and II, respectively) characterize retrograde metamorphic crystallization, whereas stage-II growth of antigorite corresponds to prograde regional metamorphism in the Archean greenstone belt. During Stage-II serpentinization, both antigorite and metamorphic olivine formed. However, the main prograde transformation in these rocks involved the breakdown of magmatic chromite. The Al, Mg and part of the Cr in the chromite diffused outward and were incorporated into the antigorite structure. In addition, hourglass-textured antigorite probably was formed during stage II, as suggested by its high Al content.

The interpretation of the original geochemical characteristics of Archean komatiites and associated rocks that have suffered several phases of metamorphism is fraught with difficulties because of multiple mineral reactions and chemical mobility. This problem was raised when komatiites were first defined (Viljoën & Viljoën 1969); these authors pointed out various modifications in the whole-rock composition of Barberton komatiites. In particular, their study stresses the importance of changes in Ca/Al ratio, which appears to decrease with increasing degree of serpentinization. In order to assess the importance of such chemical modifications, it is necessary to compare unaltered igneous assemblages with equivalent rocks that have undergone various grades of metamorphism.

The rocks of the Kuhmo belt are all metamorphosed, so that comparisons of this nature are not possible. Certain metamorphic reactions would appear to result in a simple redistribution of elements on a small scale. Thus the breakdown of chromite occurs with the loss of Al, Cr and Mg, which are fixed into antigorite. In addition, it is possible to use the chemical composition of retrograde lizardite to distinguish between igneous and metamorphic olivine: late-stage retrograde lizardite derived from metamorphic olivine is notably depleted in Al, Cr, Ni, Mn, Ca, Na and K. This criterion is supported by the textural evidence, which indicates that olivine belongs to different generations.

Acknowledgements

The authors are grateful to Drs. B.R. Frost, R.F. Martin and F.J. Wicks for their critical reviews of the manuscript and fruitful advice. The assistance and help of M. Bohn, D. Hermitte and D. Piquet with the microprobe analyses is deeply appreciated. We also acknowledge A. Falaise for her efficient typing.

References

Arndt, N.T. (1977): Thick, layered peridotite–gabbro lava flows in Munro Township, Ontario. *Can. J. Earth Sci.* **14**, 2620-2637.

______, Naldrett, A.J. & Pyke, D.R. (1977): Komatiitic and iron-rich tholeiitic lavas of Munro Township, northeast Ontario. *J. Petrol.* **18**, 319-369.

Bertrand, J.M., Blais, S. & Capdevila, R. (1978): Précisions sur l'évolution structurale de l'Archéen de Karélie (Finlande). *C.R. Acad. Sci. Paris* **287D**, 683-686.

Blais, S. (1989): Les ceintures de roches vertes archéennes de Finlande Orientale. Géologie, pétrologie, géochimie et évolution géodynamique. *Mém. Doc. du Centre Armoricain d'Étude Structurale des Socles, Rennes* **22**, 256.

______ & Auvray, B. (1987): Origine de l'olivine et du clinopyroxène dans les roches ultrabasiques komatiitiques de la ceinture archéenne de roches vertes de Kuhmo, Finlande orientale. *Bull. Minéral.* **110**, 73-92.

______, ______, Bertrand, J.M., Capdevila, R., Hameurt, J. & Vidal, P. (1977): Les grands traits géologiques de la ceinture archéenne de roches vertes de Suomussalmi–Kuhmo (Finlande orientale). *Bull. Soc. Géol. France* (7) **5**, 1033-1039.

______, ______, Capdevila, R., Jahn Bor-ming, Bertrand, J.M. & Hameurt, J. (1978): The Archaean greenstone belts of Karelia (eastern Finland) and their komatiitic and tholeiitic series. *In* Developments in Precambrian Geology: Archaean Geochemistry (B.F. Windley & S.M. Naqvi, eds.). Elsevier, Amsterdam (87-107).

Bliss, N.W. & MacLean, W.H. (1975): The paragenesis of zoned chromite from central Manitoba. *Geochim. Cosmochim. Acta* **39**, 973-990.

Boudier, F. (1971): Minéraux serpentineux extraits de péridotites serpentinisées des Alpes occidentales. *Contrib. Mineral. Petrol.* **33**, 331-345.

Echeverria, M.L. (1980): Tertiary or Mesozoic komatiites from Gorgona Island, Colombia: field relations and geochemistry. *Contrib. Mineral. Petrol.* **73**, 253-266.

Frost, B.R. (1975): Contact metamorphism of serpentinite, chloritic blackwall and rodingite at Paddy-Go-Easy Pass, central Cascades, Washington. *J. Petrol.* **16**, 272-313.

Golightly, J.P. & Arancibia, O.N. (1979): The chemical composition and infrared spectrum of nickel- and iron-substituted serpentine from a nickeliferous laterite profile, Soroako, Indonesia. *Can. Mineral.* **17**, 719-728.

Hanski, E. (1980): Komatiitic and tholeiitic metavolcanics of the Siivikkovaara area in the Archean Kuhmo greenstone belt, eastern Finland. *Bull. Geol. Soc. Finland* **52**, 67-100.

Hietanen, A. (1977): Blades of olivine in ultramafic rocks from northern Sierra Nevada, California. *J. Res. U.S. Geol. Surv.* **5**, 217-219.

Jahn Bor-ming, Auvray, B., Blais, S., Capdevila, R., Cornichet, J., Vidal, P. & Hameurt, J. (1980): Trace element geochemistry and petrogenesis of Finnish greenstone belts. *J. Petrol.* **21**, 201-244.

Laurent, R. & Hébert, Y. (1979): Paragenesis of serpentine assemblages in harzburgite tectonite and dunite cumulate from the Quebec Appalachians. *Can. Mineral.* **17**, 857-869.

Maltman, A.J. (1978): Serpentine textures in Anglesey, north Wales, United Kingdom. *Geol. Soc. Am. Bull.* **89**, 972-980.

MARTIN, H. (1985): Nature, origine et évolution d'un segment de croûte continentale archéenne: contraintes chimiques et isotopiques. Exemple de la Finlande orientale. *Mém. Doc. du Centre Armoricain d'Étude Structurale des Socles, Rennes* **1**, 392 p.

______, AUVRAY, B., BLAIS, S., CAPDEVILA, R., HAMEURT, J., JAHN BOR-MING, PIQUET, D., QUERRÉ, G. & VIDAL, P. (1984): Origin and geodynamic evolution of the Archaean crust of Eastern Finland. *Bull. Geol. Soc. Finland* **56**, 1-2, 135-160.

______, CHAUVEL, C. & JAHN BOR-MING (1983): Major and trace element geochemistry and crustal evolution of Archaean granodioritic rocks from eastern Finland. *Precambrian Res.* **21**, 159-180.

______ & QUERRÉ, G. (1984): A 2.5 Ga reworked sialic crust. Rb–Sr ages and isotopic geochemistry of late Archaean volcanic and plutonic rocks from E. Finland. *Contrib. Mineral. Petrol.* **85**, 292-299.

MOESKOPS, P.G. (1977): Serpentine minerals from two areas of the Western Australian nickel belt. *Mineral. Mag.* **41**, 313-322.

NESBITT, R.W. (1971): Skeletal crystal forms in ultramafic rocks of the Yilgarn Block, Western Australia: evidence for an Archaean ultramafic liquid. *In* Archaean Rocks (J.E. Glover, ed.). *Geol. Soc. Aust., Spec. Publ.* **3**, 331-348.

NISBET, E.G., BICKLE, M.J. & MARTIN, A. (1977: The mafic and ultramafic lavas of the Belingwe greenstone belt, Rhodesia. *J. Petrol.* **18**, 521-566.

PIIRAINEN, T. (1988): The geology of the Archaean greenstone–granitoid terrain in Kuhmo, eastern Finland. *Geol. Surv. Finland, Spec. Pap.* **4**, 39-51.

PINSENT, R.H. & HIRST, D.M. (1977): The metamorphism of the Blue River ultramafic body, Cassiar, British Colombia, Canada. *J. Petrol.* **18**, 567-594.

PIQUET, D. (1982): *Mécanismes de Recristallisations Métamorphiques dans les Ultrabasites: Exemple des Roches Vertes Archéennes de Finlande Orientale (Ceintures de Suomussalmi–Kuhmo).* Thèse 3ème cycle, Univ. Rennes, Rennes, France.

SPRINGER, R.K. (1974): Contact metamorphosed ultramafic rocks in the western Sierra Nevada Foothills, California. *J. Petrol.* **15**, 160-195.

TAIPALE, K. (1983): The geology and geochemistry of the Archaean Kuhmo greenstone–granite terrain in the Tipasjärvi area, eastern Finland. *Acta Univ. Oulu A* **151**, *Geol.* **5**, 98 p.

______, TUOKKO, I. & PIIRAINEN, T. (1980): A brief introduction in the geology and geochemistry of the Kuhmo greenstone belt, eastern Finland. *In* Nickel Sulfides in Ultramafic and Mafic Rocks (IGCP project 161, H. Papunen, ed.). Field excursion guidebook, 37-73.

THAYER, T. (1970): Chromite segregations as petrogenetic indicators. *Geol. Soc. S. Afr., Spec. Publ.* **1**, 380-390.

TROMMSDORFF, V. & EVANS, B.W. (1977): Antigorite-ophicarbonates: phase relations in a portion of the system $CaO–MgO–SiO_2–H_2O–CO_2$. *Contrib. Mineral. Petrol.* **60**, 39-56.

VIDAL, P., BLAIS, S., JAHN BOR-MING, CAPDEVILA, R. & TILTON, G.R. (1980): U–Pb and Rb–Sr systematics of the Suomussalmi Archean greenstone belt (eastern Finland). *Geochim. Cosmochim. Acta* **44**, 2033-2044.

VILJOËN, R.P. & VILJOËN, M.J. (1969): The effects of metamorphism and serpentinization of the volcanic and associated rocks of the Barberton region. *Geol. Soc. S. Afr., Spec. Publ.* **2**, 29-53.

WHITTAKER, E.J.W. & ZUSSMAN, J. (1956): The characterization of serpentine minerals by X-ray diffraction. *Mineral. Mag.* **31**, 107-126.

WICKS, F.J. & PLANT, A.G. (1979): Electron-microprobe and X-ray-microbeam studies of serpentine textures. *Can. Mineral.* **17**, 785-830.

______ & WHITTAKER, E.J.W. (1977): Serpentine textures and serpentinization. *Can. Mineral.* **15**, 459-488.

______, ______ & ZUSSMAN, J. (1977): An idealized model for serpentine textures after olivine. *Can. Mineral.* **15**, 446-458.

______ & ZUSSMAN, J. (1975): Microbeam X-ray diffraction patterns of the serpentine minerals. *Can. Mineral.* **13**, 244-258.

WINDLEY, B.F. & BRIDGWATER, D. (1971): The evolution of Archaean low- and high-grade terrains. *Geol. Soc. Aust., Spec. Publ.* **3**, 33-46.

ZHANG YIJUN (1981): Metamorphic olivine in peridotite komatiite flows, Lac Guyer, Quebec: discussion. *Can. Mineral.* **19**, 361.

Received April 22, 1987, revised manuscript accepted November 29, 1989.